Egypt. J. Chem. **Vol. 65,** No. SI:13B pp. 1129 - 1134 (2022)

Egyptian Journal of Chemistry

http://ejchem.journals.ekb.eg/

Photocatalytic Activity of Chitosan/Zn-gel Blend for the Photo Degradation of Methyl Orange, for Wastewater Treatment

H. A. Wahab [a,b*], N. Gwily [c*], D. Atta [c], I. K. Battisha [a,b]

[a] *Solid State Physics Department, Physics Research Institute, National Research Centre (NRC), Dokki, Giza, Egypt, (Affiliation ID: 60014618).*

[b] *Electric and dielectric materials measurement Unit, National Research Centre (NRC), Dokki, Giza, Egypt, (Affiliation ID: 60014618).*

[c] *Nonlinear optics unit, Spectroscopy Department, Physics Research Institute, National Research Centre, (NRC), Dokki, Giza, Egypt. (Affiliation ID: 60014618)*

Abstract

The purpose of this work was to examine the photocatalytic activity of Chitosan/Zn- gel blend film. It is well known that Chitosan can do photo-degradation; Zinc gel was added as a blend to enhance the photo-catalytic behavior of chitosan. Their photocatalytic activities were estimated by the degradation of the used dye from its solution by using the Chitosan/Zn-gel blend film. The influence of operating parameters such as Zn-gel concentration was thoroughly examined to obtain the optimum conditions for photo-catalytic degradation. The particle size for Zn-gel and the dielectric properties for Chitosan/Zn-gel blend was measured. The kinetics and color photo-degradation efficiency has been calculated based on spectrophotometry. It is found that the prepared blinds are very efficient as photo-catalytic media for the Methyl Orang; the color removal efficiency reached 87% which is great, especially since no complicated preparation followed and also no special irradiation only the sunlight The ε' and ε" were measured in a frequency range extending from 1 Hz up to 100 kHz. The frequency enhancement results in collapsing of the ε' amounts for all mentioned prepared samples and the ε' appeared independent of frequency.

Keywords: Zn gel; Chitosan; Photocatalytic activity; Methyl Orange; Spectrophotometry; Bio-material.

1. Introduction

Several vital industries including the textile industry, painting and printing industry, and cosmetics [1] are using synthetic organic compounds in the dye form to finish their products and release colored effluents in various water bodies like lakes, rivers, etc.

Those industrial synthetics were classified as one of the most dangerous, toxic, and carcinogenic recorded substances. In addition, the presence of those color centers decreases the transparency of the aquatic media, this leads to decreasing the number of sun waves penetrating the aquatic media and affecting the aquatic creatures. Those dyes are very stable chemically and did not naturally degrade. As these kinds of dyes are very important to the industry, their levels in the aquatic system increase are continuously increased. The presence of these compounds in the aquatic system increases its storage in the flesh of the aquatic creatures, which are of much concern to human and animal societies. Therefore, cleaning the aquatic systems from these kinds of chemicals could be regarded as a very important task, and it should be removed initially from the industrial wastewater before discharging into various aquatic systems [2&3]. Some of the current waste removals including filtration, adsorption, and/or chemical treatment are not effective enough for the complete removal of dyes. On the other hand, the majority of those effective methods depend either on the complicated way of fabrication like *nano*-material preparation or on expensive materials [4].

Methyl Orange (M.O.) is one of the families of dyes called AZO-dyes. M.O. is constructed of two rings connected by nitrogen atoms and ended with sulfur one. M.O. extensively applied in many industrial approaches such as food industry, textile industry, leather industry, and pharmaceutical

*Corresponding author e-mail: ha.abdelwahap@nrc.sci.eg; (Hanan A. Wahab) n_gweily@yahoo.com; (Noha Gwily).
Receive Date: 14 August 2022, Revise Date: 19 August 2022, Accept Date: 31 August 2022
DOI: 10.21608/EJCHEM.2022.156162.6759

industry. M.O. has several alternative names like acidic orange because of its sensitivity to the pH value, so it could be used to sense the presence of chlorides and hydrogen gas, or even the acidity and basicity [5-9]. Different photo-degradation methods were utilized like reverse-osmosis, coagulation, membrane, complexometric, and other many methods to overcome the presence of M.O.in aquatic media [10].

Photocatalysis could be regarded as one of the best degradation methods that seem to be a promising technique for wastewater treatment for organic compounds, especially since this method depends on utilizing sunlight or artificial illumination like UV-lamb [11–13] in the presence of a photosensitizer.

Using semiconductors as photosensitizers became in the last few decades textile contaminants removal from the wastewater [14]. In this regime, the usage of semiconductors is regarded as one of the cheap and cleaner materials in the Photocatalysis process [15-17].

ZnO is regarded as a semiconductor, and one of the most used metal oxides in the photocatalysis process, because of its high photosensitivity. ZnO also is not toxic, cheap, and eco-friendly [18, 19].

Acetylation of chitin produces Chitosan, in the last decades' Chitosan could be noticed as one of the most researched and investigated bio-materials. Chitosan could be easily soluble in water or slightly acidic water. [20-23]

Spectroscopy always plays a crucial role in analyzing any new samples, the spectroscopic tools of analysis in molecular identification such as FTIR, Raman, and molecular modeling could help assign vast spectra of samples from the archeological samples to the biological samples [24-32]. Another kind of spectroscopic tool is atomic spectroscopy like atomic absorption, ICP, and neutron activation which also help in different types of samples like soils and water treatment and biological molecules [33-36]. One of the most straightforward and powerful tools is spectrophotometry which could help enormously in measuring the concentration of such substance according to its absorption, transmission, and reflection.

Zn-gel has been studied as a photocatalyst for the removal of dyes. However, this study investigated the preparation of the Chitosan / Zn-gel blend and its effect on the degradation of M.O.

2. Experimental

2.1Preparation of Zn-gel solution:

Zinc acetate dehydrates (Zn (CH3COO)2·2H2O) from Oxford, was dissolved in mono-ethanolamine (NH2CH2CH2OH) (MEA) from Oxford, and 2-methoxy ethanol (2ME) from Merch, (mixed solution) at room temperature (about 25ºC)for preparing Zn-gel solution. The zinc acetate molar ratio to MEA was 1:1 and the zinc acetate concentration is 0.5 M. The Zn- gel solution was stirred for 2h at 50°C until yielding a homogeneous and clear solution. The mixed Zn gel solution was aged for another 24 h at room temperature.

2.2 Fabrication of the Chitosan/Zn-gel blends films:

Chitosan (deacetylated chitin, Poly (D-glucosamine)) with low molecular weight, and 75-85% deacetylated, has been bought from Sigma-Aldrich company- from Merk Group- Germany. The commercial acetic acid is 97% from Adwic-Egypt. The UV-Vis spectrophotometry has been performed using spectrophotometer model V-770 from Jasco-Japan.

200 mg of chitosan have been added to 80 ml of 7% acetic acid, then strong stirring for 5 min. the chitosan solution has been divided equally into two amounts. 1ml of Zn gel solution (CZn-1) has been added to the first chitosan solution amount and 5ml of Zn gel solution (CZn-5) added to the other amount, then another 5 min gentle stirring.

The Chitosan/Zn-gel blend thick films have been formed by the casting technique. Solution of Methyl Orang with concentration 50 µM has been prepared and piece of 2.5 by 2.5 cm of the CZn-1 and CZn-5 films have been immersed in the solution in a small beaker, the whole experiment has been done in July sun starting from noon time.

3. 3. Results and Discussion

The dielectric property of CZn films is inspiring for many reasons such as processability, cost-effectiveness, and biocompatibility. The dielectric properties of CZn-5 films depend on unexploited different factors. Only there are slight dielectric properties results for some artificial polymer blinds.

According to the percolation theory for dielectric polymer blind properties, metal oxides added to the polymeric matrix elevates its dielectric values. For a critical amount, a rapid dielectric value will be detected and specified as the percolation threshold (Pc). The dielectric evaluation needs useful information for electric field applied and distribution, chemical bonds, charge transportation mechanism of the used sample, and polarization mechanism. The most interesting dielectric property is the complex permittivity which is given by the following relation:

$$\varepsilon^*(\omega) = \varepsilon'(\omega) + \iota\, \varepsilon''(\omega) \qquad \text{Eq 1.}$$

Where the real part of the complex dielectric constant (ε′) is called the permittivity and the imaginary part is called the dielectric loss (ε″) that originates from the friction of the dipole moments.

Experimentally ε′ can be determined using the following relation:

$$\varepsilon' = (C \times d)/(A \times \varepsilon_o) \qquad \text{Eq 2.}$$

Where $\varepsilon_{o\ is}$ the permittivity of free space, C is the measured sample capacitance given in Farad, A is the sample cross-sectional area, and d is the sample thickness in meters. While ε″ can be determined using the following relation:

$$\varepsilon'' = \varepsilon' \tan(\delta)$$

Where tan (δ) is the dissipation factor.

Figures 1 & 2 detect the Frequency dependence of ε′ and ε″ for CZn-5 before and after photo-degradation measurements. The ε′ and ε″ were measured in a frequency range extending from 1 Hz up to 100 kHz.

The obtained data reveal that the mentioned samples follow the known trends, where ε′ and ε″ decrease by increasing the frequency. The frequency enhancement results in collapsing of the ε′ amounts for all mentioned prepared samples and the ε′ appeared independent of frequency.

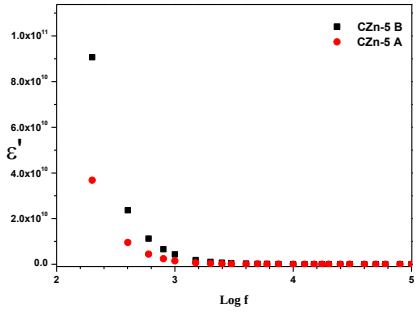

Fig 1. The Dielectric constant (ε') for CZn-5 films before and after photodegradation measurements.

The measured ε′ can be attributed to the existence of permanent electrical dipoles in the CZn-5 A and B that came from charged pairs due to the negatively charged Q and positively charged metal cations groups. By increasing the frequency, the dipoles can hardly follow the oscillations of the electric field and one can detect the collapsing of the ε′ and ε″ values. At high frequency, dipolar polarization cannot follow the oscillations electric field moreover, the ε′ become independent of frequency.

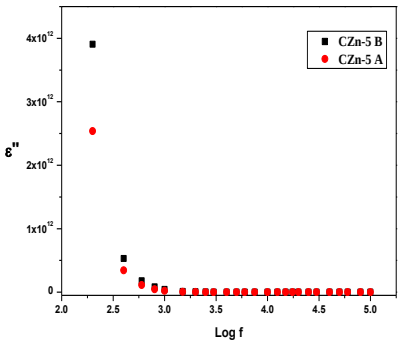

Fig 2.The Dielectric loss (ε″) for CZn-5 films before and after photodegradation measurements.

The dielectric properties enhancement of CZn films is attributed to the different development types of polarizations in the prepared films. Large defects number were contained in composite materials interfaces, resulting in charge distributions unequal which, pave way for polarizations space charge in case an electric field is presented. The continuous permittivity decrease with frequency increase is very common for all-dielectric materials. When electric field frequency is increased the polarization mechanism cannot be able to follow the change in the electric field and therefore, the polarization contribution to the dielectric constant will be diminished.

Table 1.The A. C. conductivity values for CZn-5 film before and after photodegradation measurements.

Frequency	A. C. conductivity (CZn-5) film	
	Before photodegredation	After photodegradation
2.3	23.4	5.9
3	23.36	5.1
3.6	20.1	4.7
4	10.8	3.6
4.3	2.52	1.9
5	1.06	0.22

Table 1 illustrates the A.C. conductivity values for CZn-5 film before and after photodegradation measurements. The results indicated variation in A. C. conductivity values for CZn-5 before and after measurements, especially at low frequencies. After photodegradation measurements, the CZn-5 blend film conductivity values show decreased significant changes.

3.2 Photo-degradation measurements

M.O. absorption spectra as clear in figure 3 contain two main absorption bands the highest band comes at 462nm and could be assigned to the transition $n \rightarrow \pi^*$that transition takes place in by the

free doublet on the nitrogen atom and/or the sulfur atom of C=N and/or S=C bond. Another band could be noticed at 280nm which could be attributed to the $\pi \rightarrow \pi^*$ transition that takes place in the Benzene ring.

It is clear from both fig.3 a and b that the excess of Zn gel solution makes a difference that the degradation of M.O. is not only degradation on the color by breaking the C=N and S=C only, but also breaking the benzene rings bonding which is clear from the decreasing of the absorption band at 280 nm.

Both concentrations make approximately complete degradation but the sample CZn-5 succeeded in doing the business in less than 3 hours which is promising to do the degradation in industrial west bonds.

Table2. The beak height of the bands at 462 nm and 280 nm.

Time (min)	Beak height (au)			
	1 ml		5ml	
	280 (nm)	462 (nm)	280 (nm)	462 (nm)
0	0.224	0.215	0.224	0.215
5	0.219	0.211	0.205	0.16
10	0.212	0.204	0.194	0.147
15	0.207	0.2	0.182	0.127
30	0.184	0.177	0.166	0.099
60	0.161	0.154	0.162	0.077
120	0.149	0.143	0.151	0.048
180	0.092	0.088	0.145	0.036
300	0.055	0.053	0.146	0.029

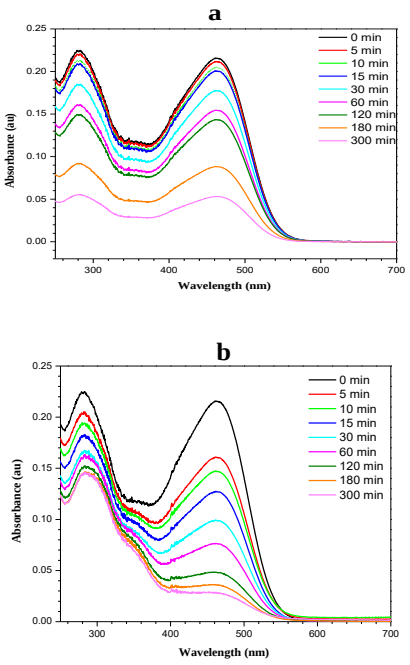

Fig. 3 The absorption spectra of M.O. after immersing samples a) CZn-1, b) CZn-5. For 0, 5, 10, 15, 30, 60, 120, 180, and 300 min.

To evaluate the performance of the prepared blind films we need to calculate the color removal efficiency (h) in terms of the concentration of M.O. before treating (Co) and the end concentration (C) as [37]

$$\eta = (C_0 - C)/C_0 \qquad \text{Eq 3.}$$

One of the most important parameters is the degradation reaction kinetics from starting concentration C_o to the end concentration after time t. that kinetics could be evaluated using the apparent first-order kinetics model, by following the rate of the M.O. degradation at 462 nm in terms of the time consumed during the degradation reaction and apparent reaction time (t) in the next exponential formula [38]:

$$C=C_o\, e^{-kt} \qquad \text{Eq 4.}$$

To calculate the concentration of M.O. with time calibration curve has been illustrated and linear fitting has been done. The calibration equation has been used to calculate the concentration of M.O. the values have been tabulated in table 3.

The calibration equation was

$$Abs=0.00449*C \qquad \text{Eq 5.}$$

Table 3.The concentration of the withdrawn samples for the band 462 nm

Time (min)	Peak height (au)			
	1 ml		5 ml	
	462 (nm)	Conc. (µM)	462 (nm)	Conc. (µM)
0	0.215	49.9	0.215	49.9
5	0.211	47	0.16	35.63
10	0.204	45.43	0.147	32.74
15	0.2	44.54	0.127	28.29
30	0.177	39.42	0.099	22.05
60	0.154	34.3	0.077	17.15
120	0.143	31.85	0.048	10.69
180	0.088	19.6	0.036	8.02
300	0.053	11.8	0.029	6.46

To calculate the removal efficiency (η) equation 3 could be applied. In this regime to not busser the reader it is better to only present the data from the removing system which was the 5ml one. Hence the removal (color degradation) efficiency η = 87%.

The apparent first-order kinetics could be understood in figure 4. The data in figure 4 have been plotted from the values of ln(C_o/C) against the time as tabulated in table 4

Table 4. The values of ln(Co/C) against time.

Time (min)	ln(Co/C)
5	0.336833
10	0.421423
15	0.567513
30	0.816708

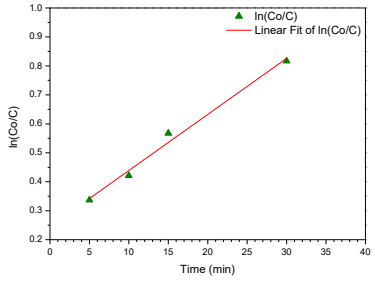

Fig. 4.The kinetics of M.O degradation by CZn-5.

In the kinetics plot, we only use the measured concentrations for 30 minutes because after 30 min. the absorbance went under 0.1 and it is known that the beer-lambert law is linear only if the absorbance values were in-between 0.1 and 0.8[39].

The kinetics of the methyl orange degradation by CZn-5 follow firmly the pseudo-first-order kinetic de-colorization, hence one could use the Langmuir-Hinshelwood model to explain that photo-catalytic process.

The advance of this method is that it did not use any additional chemicals such as H2O2 [40] or any other chemicals to reach this level of removal. Also, the usage of chemicals in bulk not in *nano* size makes it very easy and straightforward to produce the chitosan blinds at the industrial level without any complications.

4. Conclusion

This method of photodegradation is very promising that it achieved several successes, first the preparation is very easy, and simple, and not use expensive chemicals. The process did not require any special illumination like UV lamps, but only sunlight. Only two hours is enough to do the business if the used surface were enlarged. It is a promising photodegradation process to do business in the industrial west water scale but some modification to the system should be performed.

5. Conflict of Interest:

The authors declare that there are no conflicts to declare.

6. References

[1] Isai K. A. and Shrivastava V. S.,Photocatalytic degradation of methylene blue using ZnO and 2%Fe–ZnO semiconductor nanomaterials synthesized by sol–gel method: a comparative study.Springer Nature Switzerland AG, 1, 1274 (2019).

[2] Chebor L. J., Characterization of synthesized ZnO nanoparticles and their application in photodegradation of methyl orange dye under fluorescent lamp irradiation. Int J SciEngSci 2:5–8(2018).

[3] Hossain A., Sadique R.A.B.M., Raihan M. J., Nargis A., Ismail I. M. I., Habib A. and Mahmood A. J., Kinetics of degradation of eosin y by one of the advanced oxidation processes (AOPs)-Fenton's process. Am J Anal Chem 7:863–879(2016).

[4] Abebe B., Om Prakash. Y. and Tania D., Photocatalytic degradation of methylene blue dye by zinc oxide nanoparticles obtained from precipitation and sol-gel methods. Environ SciPollut Res,23: 25485–25493(2016).

[5] Choudhary B., Goyal A. and KhokraL. S., New visible spectrophotometric method for estimation of itopride hydrochloride from tablets formulations using methyl orange reagent. International Journal of Pharmacy and Pharmaceutical Sciences 1: 159- 162 (2009).

[6] Konstantinou I. K. and Albanis T. A., TiO_2-assisted photocatalytic degradation of azo dyes in aqueous solution: kinetic and mechanistic investigations: a re-view. Appl Catal B Environ, 49(1):1–14(2004) https://doi.org/10.1016/j.apcatb.2003.11.010 17.

[7] Biswas P. and Wu C-Y., Nanoparticles and the environment. Journal of the Air & Waste Management Association, 55.6: 708-746(2005), https://doi.org/10.1080/10473289.2005.10464656.

[8] Ahmad A., Mohd-Setapar SH., Chuong C. S., Khatoon A., Wani W. A., Kumar R. and Rafatullah M., Recent advances in new generation dye removal technologies: novel search for approaches to reprocess wastewater. RSC Advances 5.39: 30801-30818 (2015), https://doi.org/10.1039/C4RA16959J.

[9] Slokar M. Y. and Marechal M. L. A., Methods of decoloration of textile wastewaters. J. Dyes and pigments, 37.4: 335-356(1998), https://doi.org/10.1016/S0143-7208(97)00075-2.

[10] Riaz U., Ashraf S. and Aqib M., Microwave-assisted degradation of acid orange using a conjugated polymer, polyaniline, as catalyst. Arab. J. Chem. 7, 79–86 (2014), https://doi.org/10.1016/j.arabjc.2013.07.001.

[11] Shahabuddin S., Sarih N. M., Ismail F.H., Shahid MM and Huang N. M., Synthesis of chitosan grafted polyaniline/Co3O4 nanocube nanocomposites and their photocatalytic activity toward methylene blue dye degradation. J. RSC Adv. 5, 83857–83867 (2015), https://doi.org/10.1039/C5RA11237K.

[12] Zhou M., Han D., Liu X., Ma C., Wang H., Tang Y., Huo P., ShiW., Yan Y., and Yang J., Enhanced visible light photocatalytic activity of alkaline earth metal ions-doped CdSe/RGO photocatalysts synthesized by hydrothermal method. J. Appl. Catal. B, 172, 174–184 (2015), https://doi.org/10.1016/j.apcatb.2015.01.004.

[13] Gardin S., Signorini R., Pistore A., Giustina G. D., Brusatin G., Guglielmi M., and Bozio R., Photocatalytic Performance of Hybrid SiO2− TiO2 Films. The Journal of Physical Chemistry C114, 17, 7646-7652 (2010), https://doi.org/10.1021/jp911495h.

[14] Isai K. A and Shrivastava V. S., Detection and identification of organics and metals from industrial wastewater by ICP-AES, FTIR and GC-MS. J Adv Chem Sci 1:164–166(2015).

[15] Dey T., Nanotechnology for water purification. Chapters 6 and 7, Universal Publishers, Boca Raton, FL, USA ISBN: 1612336191(2012).

[16] Danion A., Disdier J., Guillard C and Jaffrezic-Renault N., Malic acid photocatalyticdegradationusinga TiO2-coated opticalfiber reactor. J Photochemistry and Photobiology,A Chemistry 190:135–140(2007).

[17] RaufM. A., Bukallah S. B., Hamadi A., Sulaiman A and Hammadi F., The effect of operational parameters on the

photoinduced decoloration of dyes using a hybrid catalyst V2O5/TiO2. J Chemical Engineering, 129:167–172(2007).
[18] Nibret A., Yadav O. P., Diaz I and Taddesse A. M., Cr-N Co-doped ZnO nanoparticles: synthesis, characterization and photo-catalytic activity for degradation of thymol blue. J. Bull Chem Soc Ethiopia 29, (2): 247–258(2015).
[19] Guesh K., Yadav O. P and Tadesse A., Effect of Ag-N co-doping in nanosize TiO2 on photocatalytic degradation of methyl orange dye. J Surface Science and Technol, 29:1–14(2013).
[20] Karim Z., Mathew A. P., Grahn M., Mouzon Jand Oksman K., Nanoporous membranes with cellulose nanocrystals as functional entity in chitosan: removal of dyes from water. J. Carbohydr Polym, 112:668–676 (2014).
[21] Alzahrani E., Fabrication and characterisation of chitosan-magnetic nanoparticles and its application for protein extraction. Int J AdvSci Tech Res, 4:755–766(2014).
[22] Ge J., Yue P., Chi J., Liang J andGao X., Formation and stability of anthocyanins-loaded nanocomplexes prepared with chitosan hydrochloride and carboxymethyl chitosan. J. Food Hydrocol, 74:23–31 (2018).
[23] Ren L., Yan X., Zhou J., Tong J and Su X.,Influence of chitosan concentration on mechanical and barrier properties of corn starch/chitosan films. Int J BiolMacromol, 105:1636–1643(2017).
[24] Atta D., Ismail M.M and BattishaI.K., 3D laser Raman micro-spectroscopy of Er3+ and Yb3+ co-activated nano-composite phosphosilicate for industrial photonics applications. Optics and Laser Technologythis link is disabled, 149, 107761(2022), https://doi.org/10.1016/j.optlastec.2021.107761.
[25] Refaat A., Atta D., Osman O., Mahmoud A., El-Kohadary S., Malek W., Ferretti M., Elhaes H andIbrahim M.,Analytical and computational study of three coptic icons in saint mercurius monastery, Egypt. Biointerface Research in Applied Chemistry, 9, 4685–4698 (2019), https://doi.org/10.33263/BRIAC96.685698.
[26] Farrage N.M., Oraby A.H., Abdelrazek E.M. and Atta, D., Molecular Electrostatic Potential Mapping for PANI Emeraldine Salts and Ag@PANI core-shell, Egyptian Journal of Chemistry, 62, 99–109 (2019), https://doi.org/10.21608/EJCHEM.2019.12746.1791.
[27] Atta D., Mahmoud A.E. and Fakhry A.,Protein structure from the essential amino acids to the 3D structure. Biointerface Research in Applied Chemistry, 9, 3817–3824(2019), https://doi.org/10.33263/BRIAC91.817824.
[28] Atta D., Okasha A and Ibrahim M., Setting up and calibration of simultaneous dual color wide field microscope for single molecule imaging. Der PharmaChemica, 8, 76–201682.
[29] Ibrahim M., Elhaes H. and Atta D.,Computational notes on the effect of sodium substitution on the physical properties of fullerene, Journal of Computational and Theoretical Nanoscience, 14, 4114–4117 (2017), https://doi.org/10.1166/jctn.2017.6794.
[30] Atta D., Fakhry A. and Ibrahim M.,Chitosan membrane as an oil carrier: Spectroscopic and modeling analyses. J. Der PharmaChemica, 7, 357–361 (2015).
[31] Atta D., Gomaa F., Elhaes H. and Ibrahim, M., Effect of hydrated dioxin on the physical and geometrical parameters of some amino acids. Journal of Computational and Theoretical Nanoscience. 14, 2405–2408 (2017) https://doi.org/10.1166/jctn.2017.6840.
[32] Osman O., Mahmoud A., Atta D., Okasha A. and Ibrahim, M.,Computational notes on the effect of solvation on the electronic properties of glycine. Der PharmaChemica, 7, 377–380 (2015).
[33] Farrage N.M., Oraby A.H., Abdelrazek E.M.M. and Atta, D.,Synthesis, characterization of Ag@PANI core-shell nanostructures using solid state polymerization method. Biointerface Research in Applied Chemistry, 9, 3934–3941 (2019), https://doi.org/10.33263/BRIAC93.934941.
[34] Atta D. and Okasha O., Single molecule laser spectroscopy, Spectrochimica Acta A, 135, 1173-1179 (2015), https://doi.org/10.1016/j.saa.2014.07.085.
[35] Elbanna A., Atta D. and Sherief D., In vitro bioactivity of newly introduced dual-cured resin-modified calcium silicate cement. Dental Research Journal, 19, 1 (2022), https://doi.org/10.4103/1735-3327.336686.
[36] Okasha A., Atta D., Badawy W.M.,Frontasyeva M., Elhaes H. and Ibrahim M., Modeling the coordination between Na, Mg, Ca, Fe, Ni, and Zn with organic acids.Journal of Computational and Theoretical Nanoscience, 14(3), 1357–1361(2017), https://doi.org/10.1166/jctn.2017.6457.
[37] Ming.hua Z., Qi-zhou D., Le-cheng L. and Da-hui W., Synergetic effects for p-nitrophenol abatement using a combined activated carbon adsorption-electrooxidation process. Zhejiang Univ. SCI, 5, 1512-1516 (2004), https://doi.org/10.1631/jzus.2004.1512.
[38] Nu´nez L., Garc´ıa-Hortal J. A. and Torrades F., Study of kinetic parameters related to the decolourization and mineralization of reactive dyes from textile dyeing using Fenton and photo-Fenton processes. J. Dyes and Pigments, 75, 3, 647-652 (2007), https://doi.org/10.1016/j.dyepig.2006.07.014.
[39] Thomas Wenzel., Molecular and Atomic Spectroscopy. https://chem.libretexts.org/Bookshelves/Analytical_Chemistry/Molecular_and_Atomic_Spectroscopy_(Wenzel)/1%3A_General_Background_on_Molecular_Spectroscopy/1.2%3A_Beers_Law.
[40] Melgoza D., Hern A., ırez A. and Peralta-Hernandez J. M., Comparative efficiencies of the decolourisation of Methylene Blue using Fenton's and photo-Fenton's reactions. J. Photochem. Photobiol. Sci, 8, 596–599 (2009), https://doi.org/10.1039/b817287k.